Journal of Applied Physics

Fabrication and characterization of graphene-based paper for heat spreader applications

Cite as: J. Appl. Phys. **126**, 155109 (2019); https://doi.org/10.1063/1.5097000
Submitted: 21 March 2019 . Accepted: 02 October 2019 . Published Online: 18 October 2019

Ali A. Muhsan, and Khalid Lafdi

Journal of Applied Physics | ARTICLE | scitation.org/journal/jap

Fabrication and characterization of graphene-based paper for heat spreader applications

Cite as: J. Appl. Phys. **126**, 155109 (2019); doi: 10.1063/1.5097000
Submitted: 21 March 2019 · Accepted: 2 October 2019 ·
Published Online: 18 October 2019

View Online Export Citation CrossMark

Ali A. Muhsan[1,2,a)] and Khalid Lafdi[1]

AFFILIATIONS

[1]Department of Chemical and Materials Engineering, University of Dayton, Dayton, Ohio 45469, USA
[2]Department of Materials Engineering, University of Technology, Baghdad 10066, Iraq

[a)]**Author to whom correspondence should be addressed:** muhsana1@udayton.edu

ABSTRACT

In this work, in-plane thermal conductivity measurement was carried out on graphene-based papers. Graphene-based papers were fabricated using various processing techniques such as chemical vapor deposition (CVD), hot pressing of graphene slurry, and evaporation induced self-assembly. The prepared materials were characterized using scanning electron microscopy, Raman spectroscopy, and X-ray diffraction. In-plane thermal conductivity measurement was performed via a steady state thin film thermal conductivity apparatus. The in-plane thermal conductivity measurements show that the CVD based sample has the highest thermal conductivity. COMSOL Multiphysics was used to simulate the in-plane thermal conductivity of graphene-based papers.

INTRODUCTION

Efficient heat removal is a crucial issue for advancements in information, communication, and energy storage technologies because of increasing power densities in electronics.[1,2] Performance and reliability of modern electronics, optoelectronics, photonic devices, and systems strongly rely on effective thermal management.[3] The most effective techniques used to dissipate the heat generated in electronic devices are thermal interface materials (TIMs) and lateral heat spreaders.[4,5] Graphene has intensively been used as novel carbon nanofillers to enhance the thermal conductivities of polymeric composites as TIMs.[6–8] Lateral heat spreaders function by removing local hot spots via transferring heat along the basal plane of the material.[9] These heat spreaders are widely used in various commercial portable electronic devices, such as smart phones, touch panels, and LED lamps, with more condense packed integrated circuits.[10] Graphitized polyamide paper and flexible graphite paper are typical commercial paperlike lateral heat spreaders, and their thermal conductivity is between 100 and 700 $W\,m^{-1}\,K^{-1}$.[11] Recently, free-standing graphene papers have attracted much interest in the thermal management field due to their high thermal conductivity, superior electrical conductivity, and excellent mechanical properties.[12–14] Compared with the metals commonly used for heat dissipation, free-standing graphene paper possesses ultrahigh thermal conductivity, a much lower density (<1 g/cm^3), excellent flexibility, and lower cost, signifying the potential for effective heat dissipation.[15] Numerous studies have been carried out to fabricate graphene papers with high thermal conductivity. Nevertheless, it is noted that through different synthesis methods, graphene papers achieve substantially dissimilar thermal conductivity.[16]

The techniques used to fabricate graphene papers are vacuum filtration,[17–25] evaporation induced self-assembly (EISA),[26,27] spin coating,[28] drop-casting,[29] Langmuir-Blodgett (L-B),[30] spraying,[31] dip coating,[32] Langmuir-Schaefer,[33] centrifugation,[34] mold-casting,[35,36] inkjet printing,[37,38] and pressing of graphene-containing suspension.[39] Balandin *et al.* measured the in-plane thermal conductivity of suspended single-layer graphene (4800–5300 $W\,m^{-1}\,K^{-1}$) using the optothermal Raman technique.[40] Kargar *et al.* investigated the effect of graphene fillers on electromagnetic interference shielding and thermal management of epoxy-based composites. The thermal conductivity of graphene fillers/epoxy composites was 8 $W\,m^{-1}\,k^{-1}$ calculated using the laser flash technique. They reported the optimization of proper lateral dimensions, thickness, and aspect ratio of graphene fillers for enhancing the dual functionality of graphene fillers/epoxy composites.[41] Malekpour *et al.* investigated the thermal conductivity of graphene laminate films deposited on polyethylene terephthalate using the optothermal Raman technique. The thermal conductivity measurements were in the range of 40–90 $W\,m^{-1}\,k^{-1}$. They stated that the average size and the alignment of graphene flakes affected the thermal conductivity of graphene laminate films.[42] Xiang and Drzal utilized a thermally exfoliated graphite intercalation compound, followed by filtration, annealing, and compression. The resultant reduced graphene oxide (GO) paper showed an electrical conductivity of 880 S cm^{-1} and a thermal conductivity of 200 W m^{-1} K^{-1}.[43] Kong *et al.* synthesized a hierarchical graphene/carbon fiber (CF) composite paper using the vacuum filtration technique, and they reported a thermal conductivity value of 977 W m^{-1} K^{-1}.[44] Xin *et al.* fabricated graphene papers by using the direct electro-spray deposition (ESD) technique on an aluminum foil followed by mechanical compaction and thermal annealing treatment. They reported the influence of annealing temperature on the thermal and electrical conductivity of graphene paper. At annealing temperature 2200 °C the thermal conductivity was ∼1238.3 W m^{-1} K^{-1} and the electrical conductivity was $\sim 1.57 \times 10^5$ S m^{-1}. At annealing temperature 1800 °C, the thermal and electrical conductivity were ∼809.5 W m^{-1} K^{-1} and $\sim 8.48 \times 10^4$ S m^{-1}, respectively.[45] Song *et al.* studied the role of the thermal reduction at different annealing temperatures on the thermal conductivity and tensile strength of graphene films. They showed that the highest in-plane thermal conductivity obtained at 1200 °C was 1043.5 W m^{-1} K^{-1}.[46] In this work, we prepared graphene-based papers by chemical vapor deposition (CVD), hot pressing of graphene slurry, and EISA. In-plane thermal conductivity measurement was carried out in order to determine which process would be relevant for heat spreader applications of electronic devices.

SAMPLE FABRICATION METHODS

The electrochemical exfoliation technique was used to prepare graphene oxide, which was utilized to fabricate a graphene oxide paper via the EISA method. EISA involved the dispersion of exfoliated graphene oxide suspension (6 mg/1 ml de-ionized water) by using an ultrasonic bath (BRANSON 5100) for 1 h by pouring the graphene oxide suspension in the drying tray then keeping it at room temperature for evaporation of water and self-assembled graphene oxide sheets. The thickness of the prepared graphene oxide paper is based on the volume of the suspension used. The mechanism of EISA involved the following stages: stage I: slow evaporation of the graphene oxide suspension to remove water molecules; stage II: during evaporation, the graphene oxide sheets bonded with each other through van der Waals force; stage III: finally, the bonded GO sheets connected along the drying tray to make the GO paper. The thickness of the prepared graphene oxide paper was 0.05 mm. Graphene oxide paper was reduced via the thermal annealing treatment approach to obtain the graphene paper. Thermal annealing treatment was performed in a tube furnace that involved heating the graphene oxide paper to 700 °C with a heating rate of 5 °C/min and then was held for 30 min under argon gas with a flow rate of 20 mm/min. This treatment aimed to remove the oxygen functional groups and recover sp^2 carbon–carbon bonds. The chemical vapor deposition technique was utilized to prepare the graphene-based paper.[47] Pyrolytic graphite (PG) is grown on a mandrel by chemical vapor deposition of hydrocarbon decomposition. The graphene layer is deposited by cracking methane and hydrogen at 2000 °C at a reduced pressure of 3 Torr followed by a subsequent annealing around 3000 °C. Hot pressing of graphene slurry was used to prepare the graphene-based paper. Carbon paper was prepared in the form of a thin foil made of 100% graphene. A graphene foil is made into paperlike materials using three steps: First, natural graphite was exfoliated using a traditional intercalation process. Then, the graphene nanoplatelets were oxidized using both acids and oxygen plasma. As a result, graphene oxide (GO) was fabricated with edge oxygen functional groups. Second, the GO was dispersed into water with 2% polyvinyl alcohol (PVA) and was both mechanically and ultrasonically stirred for 2 h. Once the suspension was homogenized, it was filtered using the vacuum filtration method forming an even filtered cake. Third, the cake was hot pressed in a silicon mold at a temperature of 60 °C and a pressure of 80 psi for a period of 30 min. Once the pressure is released, the material appeared very glossy with a metal shiny look.

EXPERIMENTAL METHODS AND RESULTS

A graphene-based paper was characterized using scanning electron microscopy (SEM) to determine the morphology of the graphene-based paper via the different techniques used. X-ray diffraction is performed using Rigaku Smartlab, and the operating conditions were 40 KV, 44 mA, and a scanning step of 0.04°. Raman spectroscopy was conducted via an INVIA RENISHAW Raman Microscope with laser excitation at 633 nm.

Analysis methodology

An in-plane steady state thin film thermal conductivity device was used to measure the thermal conductivity of the fabricated graphene-based papers.[48] The home-built device consisted of a power supply, a nickel film that worked as a heater and sensor, a mica film placed between the heater and graphene paper, a digital thermometer, and a vacuum chamber to avoid heat loss by convection. Figure 1 depicts the experimental setup for the in-plane thermal conductivity device used to measure the thermal conductivity of graphene-based papers. The device was calibrated using a copper film to ensure the accuracy of thermal conductivity measurements. Thermal conductivity can be calculated directly via Eq. (1) as

$$k_f = \frac{QL_f}{2\, d_f\, (T_{f,1} - T_{f,2})}, \tag{1}$$

where Q is the power dissipated in the metallic heater per unit length;

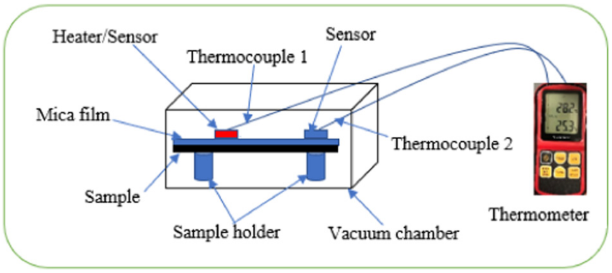

FIG. 1. Experimental setup for the in-plane thermal conductivity device.

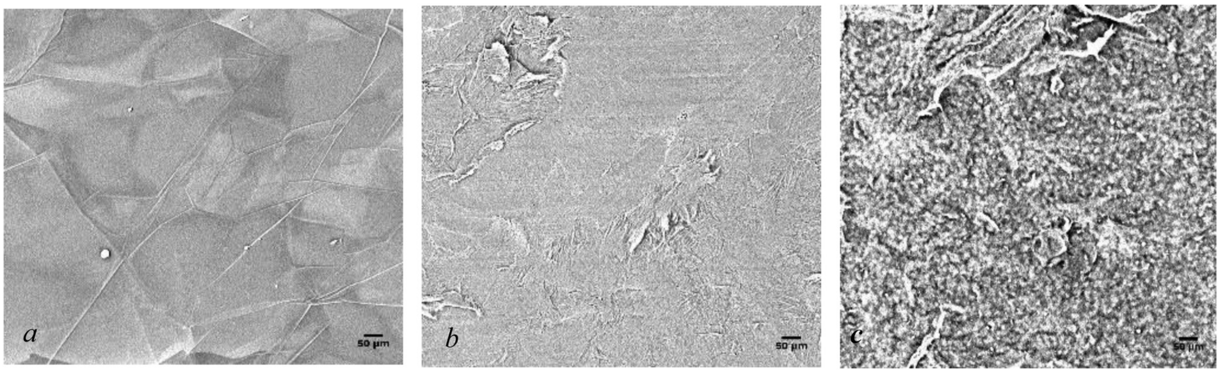

FIG. 2. SEM for graphene-based papers: (a) CVD, (b) hot pressing method, and (c) EISA method.

$L_f/2$ is the distance from the heater to the heat sink, d_f is the thickness of the graphene-based paper, $T_{f,1}$ is the thin film temperature right underneath the heater/sensor, which is assumed to be the same temperature as the heater/sensor, and $T_{f,2}$ is the temperature of the thin film edge in contact with the substrate.

Electrical conductivity of the graphene-based paper was measured using MCP-T610 (Chemical AnalyTech) via the 4 pins method.

Thermal conductivity simulation

The simulation of in-plane thermal conductivity of the graphene-based paper was studied using COMSOL Multiphysics 5.2a. The heat transfer in solid physics was used in this simulation to show the temperature gradient through graphene-based papers. Equations (2) and (3)[49] were used to solve this simulation,

$$d_z\ \rho C_p\ \frac{dT}{dt} + \nabla \cdot q = d_z\ Q + q_o + d_z\ Q_{ted}, \tag{2}$$

$$q = -d_z\ k \nabla T, \tag{3}$$

where d_z is the thickness of the graphene-based paper, ρ is the density (kg/m^3), C_p is the specific heat capacity at a constant pressure [J/(kg k)], q is the heat flux (W/m^2), Q is the heat source (W/m^3), Q_{ted} is the thermoelastic damping (this parameter is ignored because there is no thermal expansion in the simulation), k is the thermal conductivity (W m^{-1} k^{-1}) of the graphene-based paper, and ∇T is the temperature gradient. The boundary conditions are represented by the thermal insulation at the edge of the samples. Then, the meshed model was solved numerically to simulate the temperature distribution through the graphene-based paper.

Material microstructure characterization

The techniques used to fabricate the graphene-based paper's influence on the morphology and thermal conductivity of the prepared graphene-based paper because of the preparation conditions. Figure 2 shows the morphology of graphene-based papers. Figure 2(a) indicates the morphology of graphene paper prepared via the CVD technique, which showed a smooth and fine morphology because of the conditions of fabrication that involved the deposition of carbon atoms to create a thin layer of graphene and then

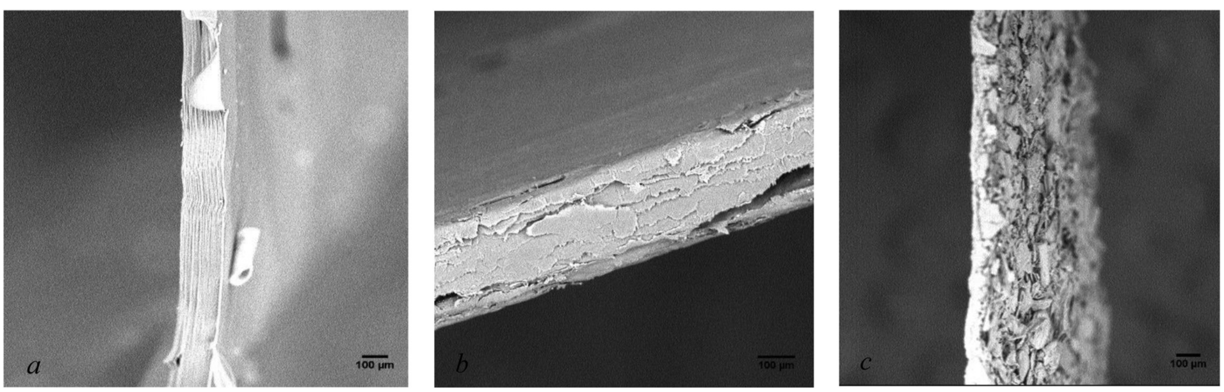

FIG. 3. SEM for cross-sectional graphene-based papers: (a) CVD, (b) hot pressing method, and (c) EISA method.

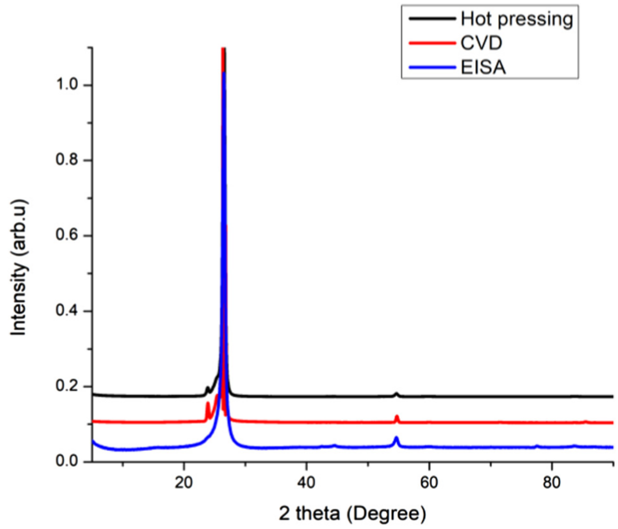

FIG. 4. X-ray patterns of graphene-based papers for the different techniques used.

subjected for annealing treatment at 3000 °C. Figures 2(b) and 2(c) show the morphology of the graphene-based paper prepared using the hot pressing and EISA methods, respectively. The structure is corrugated because it consisted of bonding of exfoliated graphene oxide. The cross section of graphene-based papers is shown in Fig. 3. Figure 3(a) shows the multilayers of the graphene film deposited by the CVD technique, which appeared very uniform. On the other hand, Fig. 3(b) shows the structure of the graphene paper, which consisted of the graphene slurry that was hot pressed to form the paper. The graphene sheets are bonded to each other to form a free-standing graphene paper as shown in Fig. 3(c).

As shown in Fig. 4, graphene-based papers have the same X-ray profile. As indicated in this figure, they have a sharp peak at 26.6° corresponding to the (002) plane with a d-interspacing of 3.36 Å. The orientation of graphene-based papers was characterized utilizing Rigaku Oxford X-ray diffraction. Figure 5 shows the small angle X-ray scattering (SAXS), which indicated that the CVD method has the highest orientation for the prepared graphene-based papers, while the EISA method led to a less oriented graphene membrane due to the conditions of preparation that were based on self-assembly of graphene sheets as illustrated in Fig. 5(c). As shown in Fig. 5(a), a small arc was apparent. It seems very clear that the graphene-based paper made via the CVD method exhibits high orientation and crystallinity. However, only a ring and a large arc (misorientation) indicated a partial orientation of the graphene-based paper made via the hot pressing method as shown in Fig. 5(b).

The quality of the graphene-based paper was determined via Raman spectroscopy. The D peak originates from the breathing mode of six-atom rings and requires a defect for activation; therefore, the intensity of the D peak depends on the disorder of the graphene. The 2D peak is the second order of the D peak, and the shape of the 2D peak varies with different thicknesses of several layers of graphene sheets.[50] The G peak represents the E_{2g} phonon vibration mode in the center of the Brillouin zone of an sp^2 hybrid carbon atom. Figure 6 shows the Raman spectra for the prepared graphene-based papers via different techniques.

Graphene-based papers that were fabricated by using the CVD and hot pressing techniques have higher quality due to the disappearance of the D peak. As shown in Fig. 6, the D peak appeared in the graphene-based paper prepared via the EISA technique due to the exfoliated graphene oxide defects.

Thermal conductivity measurements

The thermal conductivity of prepared graphene-based paper is entirely affected by the technique used and the presence of defects that have an effect on the phonon dispersion. The thermal conductivity of the graphene-based paper prepared via the CVD technique, hot pressing , and the EISA method were 1293 W m^{-1} k^{-1}, 983 W m^{-1} k^{-1}, 563 W m^{-1} k^{-1}, respectively, as shown in Table I. On a prior work, Renteria *et al.* measured the in-plane thermal conductivity 61 W m^{-1} k^{-1} for reduced graphene film annealed at 1000 °C. They reported that the phonon thermal transport is

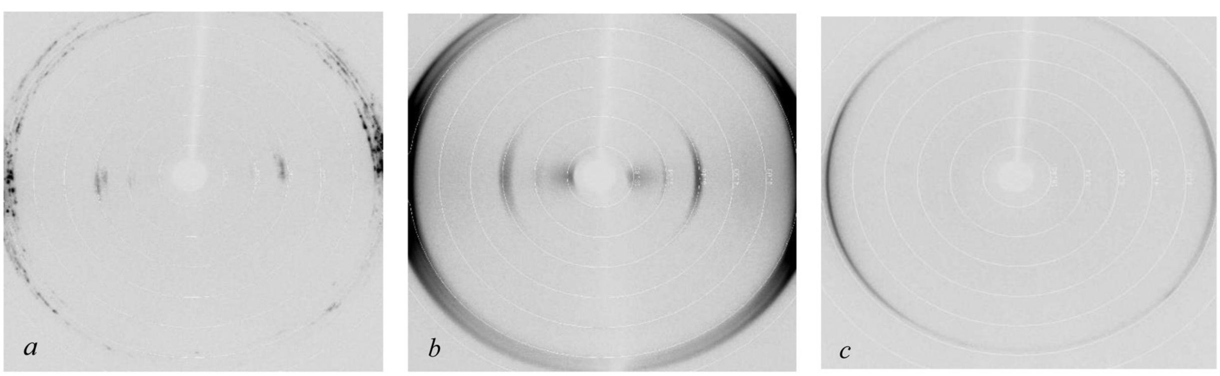

FIG. 5. SAXS images for graphene-based papers: (a) CVD, (b) hot pressing, and (c) EISA.

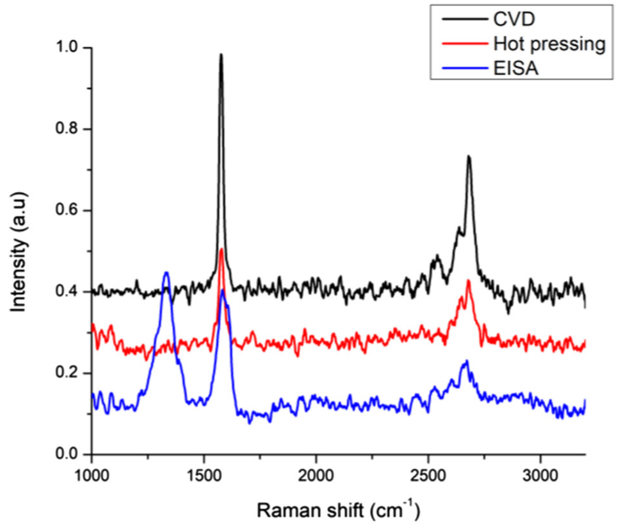

FIG. 6. Raman spectra for graphene-based papers.

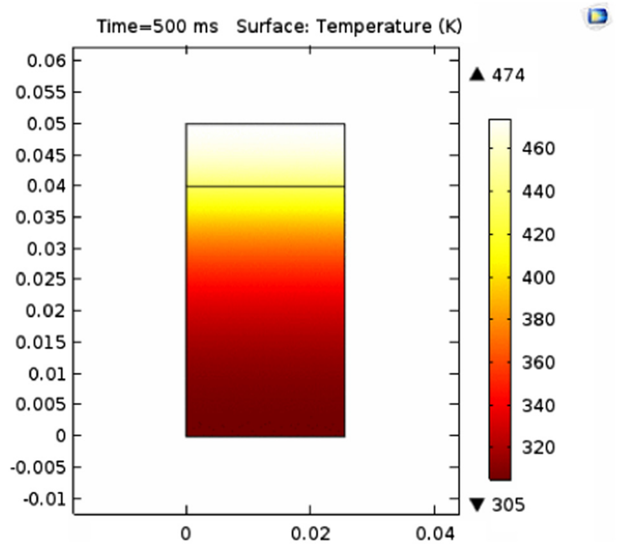

FIG. 7. Temperature gradient through the graphene-based paper prepared via CVD.

limited by the disorder and concentration of defects.[51] The highest thermal conductivity of the graphene-based paper via CVD is related to the high free mean path of phonons, which is dominated for thermal conductivity of the graphene paper. The quality of the graphene-based paper is controlled by the thermal conductivity because of the defects that influence the phonon dispersion. The alignment of graphene layers and the presence of defects have affected the measurements of thermal conductivity of the graphene-based papers. The electrical conductivity measurements of the graphene-based paper indicated the highest value of 6.4×10^6 S m^{-1} for the CVD technique. The hot pressing technique has an electrical conductivity value of 2.3×10^6 S m^{-1}, while the EISA method has a value of 3.8×10^4 S m^{-1} as shown in Table I. The techniques used played a key role on the electron mobility that affected the electrical conductivity of the graphene-based paper. The simulation of in-plane thermal conductivity for graphene-based papers showed the temperature gradient through the graphene-based paper as a function of thermal conductivity of graphene-based paper as shown in Fig. 7. The temperature dropped from the heating source toward the sink as indicated in Fig. 7. The simulation of the temperature distribution through the graphene-based paper showed the role of high thermal conductivity of the graphene paper prepared via the CVD method.

TABLE I. Thermal conductivity and electrical conductivity for the graphene-based papers.

Graphene-based papers	Thermal conductivity (W m^{-1} k^{-1})	Electrical conductivity (S m^{-1})
CVD graphene-based paper	1293	6.4×10^6
Hot pressing of graphene slurry	983	2.3×10^6
EISA graphene-based paper	563	3.8×10^4

CONCLUSION

In conclusion, in-plane thermal conductivity of graphene-based papers was totally dependent on the fabrication technique that affects their structure and quality. The EISA method is the cheapest and simplest technique than the other used techniques. However, graphene-based papers prepared via CVD and hot pressing methods have higher quality than EISA because of the presence of defects. Raman spectra showed that the D peak did not appear for the graphene-based paper fabricated via CVD and hot pressing techniques. Highest electrical conductivity was measured for the graphene-based paper fabricated by the CVD method because of its highest graphitizability and crystallite alignment. In-plane thermal conductivity values of graphene-based paper were in the order of $K_{CVD} > K_{hot\ pressing} > K_{EISA}$. The graphene-based paper prepared via the CVD technique has ultrahigh in-plane thermal conductivity, so it is more suitable for heat spreader applications. The simulation of the temperature gradient through graphene-based papers showed the role of high thermal conductivity of the graphene paper prepared via the CVD method.

ACKNOWLEDGMENTS

We declare that there are no conflicts with regard to this work.

REFERENCES

[1] A. Balandin, "Chill out," IEEE Spectr. **29**, 34–39 (2009).
[2] S. V. Garimella *et al.*, "Thermal challenges in next-generation electronic systems," IEEE Trans. Compon. Packaging Technol. **31**, 801–815 (2008).

[3]K. M. F. Shahil and A. A. Balandin, "Thermal properties of graphene and multilayer graphene: Applications in thermal interface materials," Solid State Commun. **152**(15), 1331–1340 (2012).
[4]M. M. Sadeghi, M. T. Pettes, and L. Shi, "Thermal transport in graphene," Solid State Commun. **152**, 1321 (2012).
[5]A. A. Balandin, "Thermal properties of graphene and nanostructured carbon materials," Nat. Mater. **10**, 569 (2011).
[6]W.-L. Song, L. M. Veca, C. Y. Kong, S. Ghose, J. W. Connell, P. Wang, L. Cao, Y. Lin, M. J. Meziani, H. J. Qian, G. E. LeCroy, and Y.-P. Sun, "Polymeric nanocomposites with graphene sheets—Materials and device for superior thermal transport properties," Polymer **53**, 3910–3916 (2012).
[7]T. F. Luo and J. R. Lioyd, "Enhancement of thermal energy transport across graphene/graphite and polymer interfaces: A molecular dynamics study," Adv. Funct. Mater. **22**, 2495–2502 (2012).
[8]M. Terrones, O. Martín, M. González, J. Pozuelo, B. Serrano, J. C. Cabanelas, S. M. Vega-Díaz, and J. Baselga, "Interphases in graphene polymer-based nanocomposites: Achievements and challenges," Adv. Mater. **23**, 5302–5310 (2011).
[9]S. Subrina, "Heat transport in graphene interconnect networks with graphene lateral heat spreaders," IEEE Trans. Nanotechnol. **11**, 777 (2012).
[10]Z. Yan, G. X. Liu, J. M. Khan, and A. A. Balandin, "Graphene quilts for thermal management of high power GaN transistors," Nat. Commun. **3**, 827 (2012).
[11]X. H. Wei, L. Liu, J. X. Zhang, J. L. Shi, and Q. G. Guo, "Mechanical, electrical, thermal performances and structure characteristics of flexible graphite sheets," Mater. Sci. **45**, 2449 (2010).
[12]Y. Guo, C. Dun, J. Xu, J. Mu, P. Li, L. Gu, C. Hou, C. A. Hewitt, Q. Zhang, Y. Li *et al.*, "Ultrathin, washable, and large-area graphene papers for personal thermal management," Small **13**, 1702645 (2017).
[13]T. Ma, Z. Liu, J. Wen, Y. Gao, X. Ren, H. Chen, C. Jin, X. L. Ma, N. Xu, H. M. Cheng *et al.*, "Tailoring the thermal and electrical transport properties of graphene films by grain size engineering," Nat. Commun. **8**, 14486 (2017).
[14]G. Xin, W. Zhu, T. Yao, S. M. Scott, and J. Lian, "Microstructure control of macroscopic graphene paper by electrospray deposition and its effect on thermal and electrical conductivities," Appl. Phys. Lett. **110**, 091909 (2017).
[15]C. M. Gee, C. C. Tseng, F. Y. Wu, C. T. Lin, H. P. Chang, L. J. Li, J. C. Chen, and L. H. Hu, "Few layer graphene paper from electrochemical process for heat conduction," Mater. Res. Innov. **18**, 208–213 (2014).
[16]W. Yu, H. Xie, F. Li, J. Zhao, and Z. Zhang, "Significant thermal conductivity enhancement in graphene oxide papers modified with alkaline earth metal ions," Appl. Phys. Lett. **103**, 141913 (2013).
[17]K. Dağcı and M. Alanyalıoğlu, "Preparation of free-standing and flexible graphene/Ag nanoparticles/poly (pyronin Y) hybrid paper electrode for amperometric determination of nitrite," ACS Appl. Mater. Interfaces **8**, 2713–2722 (2016).
[18]H. Gao, Y. Wang, F. Xiao, C. B. Ching, and H. Duan, "Growth of copper nanocubes on graphene paper as freestanding electrodes for direct hydrazine fuel cells," J. Phys. Chem. C **116**, 7719–7725 (2012).
[19]Y. Liu, W. Wang, L. Gu, Y. Wang, Y. Ying, Y. Mao, L. Sun, and X. Peng, "Flexible CuO nanosheets/reduced graphene oxide composite paper: Binder-free anode for high-performance lithium-Ion batteries," ACS Appl. Mater. Interfaces **5**, 9850–9855 (2013).
[20]H. P. de Oliveira, S. A. Sydlik, and T. M. Swager, "Supercapacitors from free-standing polypyrrole/graphene nanocomposites," J. Phys. Chem. C **117**, 10270–10276 (2013).
[21]D. W. Wang, F. Li, J. Zhao, W. Ren, Z. G. Chen, J. Tan *et al.*, "Fabrication of graphene/polyaniline composite paper via in situ anodic electropolymerization for high-performance flexible electrode," ACS Nano **3**, 1745–1752 (2009).
[22]Y. Hu, X. Li, J. Wang, R. Li, and X. Sun, "Free-standing graphene/carbon nanotube hybrid papers used as current collector and binder free anodes for lithium ion batteries," Power Sources **237**, 41–46 (2013).
[23]N. Zhu, S. Han, S. Gan, J. Ulstrup, and Q. Chi, "Graphene paper doped with chemically compatible prussian blue nanoparticles as nanohybrid electrocatalyst," Adv. Funct. Mater. **23**, 5297–5206 (2013).
[24]Y. Dai, S. Cai, W. Yang, L. Gao, W. Tang, J. Xie, J. Zhi, and X. Ju, "Fabrication of self-binding noble metal/flexible graphene composite paper," Carbon **50**, 4648–4654 (2012).
[25]C. Mattevi, G. Eda, S. Agnoli *et al.*, "Evolution of electrical, chemical, and structural properties of transparent and conducting chemically derived graphene thin films," Adv. Funct. Mater. **19**, 2577–2583 (2009).
[26]Z. Khan, A. Kausar, H. Ullah, A. Badshah, and W. Khan, "A review of graphene oxide, graphene buckypaper, and polymer/graphene composites: Properties and fabrication techniques," J. Plast. Film Sheeting **32**, 336–379 (2016).
[27]E. Ou, X. Zhang, Z. Chen *et al.*, "Macroscopic free-standing Ag-reduced, graphene oxide Janus films prepared by evaporation-induced self-assembly," Chem. Eur. J. **17**, 8789–8793 (2011).
[28]J. T. Robinson, M. Zalalutdinov, J. W. Baldwin *et al.*, "Wafer-scale reduced graphene oxide films for nanomechanical devices," Nano Lett. **8**, 3441–3445 (2008).
[29]H. C. Schniepp, J. L. Li, M. J. McAllister *et al.*, "Functionalized single graphene sheets derived from splitting graphite oxide," J. Phys. Chem. B **110**, 8535–8539 (2006).
[30]L. J. Cote, F. Kim, and J. Huang, "Langmuir-Blodgett assembly of graphite oxide single layers," J. Am. Chem. Soc. **131**, 1043–1049 (2008).
[31]S. Gilje, S. Han, M. Wang *et al.*, "A chemical route to graphene for device applications," Nano Lett. **7**, 3394–3398 (2007).
[32]X. Wang, L. Zhi, and K. Mullen, "Transparent, conductive graphene electrodes for dye-sensitized solar cells," Nano Lett. **8**, 323–327 (2008).
[33]R. Y. Gengler, A. Veligura, A. Enotiadis *et al.*, "Large-yield preparation of high electronic-quality graphene by a Langmuir–Schaefer approach," Small **6**, 35–39 (2010).
[34]F. Liu, Y. Piao, K. S. Choi, and T. S. Seo, "Fabrication of freestanding graphene composite films as electrochemical biosensors," Carbon **50**, 123–133 (2012).
[35]F. Xiao, Y. Li, X. Zan, K. Liao, R. Xu, and H. Duan, "Growth of metal–metal oxide nanostructures on freestanding graphene paper for flexible biosensors," Adv. Funct. Mater. **22**, 2487–2494 (2012).
[36]Y. Sun, K. He, Z. Zhang, A. Zhou, and H. Duan, "Real time electrochemical detection of hydrogen peroxide secretion in live cells by Pt nanoparticles decorated graphene–carbon nanotube hybrid paper electrode" Biosens. Bioelectron. **68**, 358–364 (2015).
[37]F. Xiao, S. Yang, Z. Zhang, H. Liu *et al.*, "Scalable synthesis of freestanding sandwich structured graphene/polyaniline/graphene nanocomposite paper for flexible all-solid-state supercapacitor," Sci. Rep. **5**, 9359 (2015).
[38]K. Chi, Z. Zhang, J. Xi, Y. Huang, F. Xiao, S. Wang, and Y. Liu, "Freestanding graphene paper supported three-dimensional porous graphene–polyaniline nanocomposite synthesized by inkjet printing and in flexible all-solid-state supercapacitor," ACS Appl. Mater. Interfaces **6**, 16312–16319 (2014).
[39]F. Liu, S. Song, D. Xue, and H. Zhang, "Folded structured graphene paper for high performance electrode materials," Adv. Mater. **24**, 1089–1094 (2012).
[40]A. A. Balandin, S. Ghosh, W. Bao, I. Calzio, D. Teweldebrhan, F. Miao, and C. N. Lua, "Superior thermal conductivity of single graphene-layer," Nano Lett. **8**, 902–907 (2008).
[41]F. Kargar, Z. Barani, M. Balinskiy, A. S. Magana, J. S. Lewis, and A. Balandin, "Dual functional graphene composites for electromagnetic shielding and thermal management," Adv. Electron. Mater. **5**, 1800558 (2019).
[42]H. Malekpour, K.-H. Chang, J.-C. Chen, C.-Y. Lu, D. L. Nika, K. S. Novoselov, and A. A. Balandin, "Thermal conductivity of graphene laminate," Nano Lett. **14**, 5155–5161 (2014).
[43]J. Xiang and L. T. Drzal, "Electron and phonon transport in Au nanoparticle decorated graphene nanoplatelet nanostructured paper," ACS Appl. Mater. Interfaces **3**, 1325–1323 (2011).
[44]Q. Kong, Z. Liu, J. Gao, C. Chen, Q. Zhang, G. Zhou, Z. Tao, X. Zhang, M. Wang, F. Li, and R. Cai, "Hierarchical graphene–carbon fiber composite paper as a flexible lateral heat spreader," Adv. Funct. Mater. **24**, 422228 (2014).
[45]G. Xin, H. Sun, T. Hu, H. Fard, X. Sun, N. Koratkar, T. Borca-Tasciuc, and J. Lian, "Large-area freestanding graphene paper for superior thermal management," Adv. Mater. **26**, 4521–4526 (2014).

[46]N.-J. Song, C.-M. Chen, C. Lu *et al.*, "Thermally reduced graphene oxide films as flexible lateral heat spreaders," J. Mater. Chem. A **2**, 16563–16568 (2014).
[47]X. Li, L. Colombo, and R. S. Ruoff, "Synthesis of graphene films on copper foils by chemical vapor deposition," Adv. Mater. **28**, 6247–6252 (2016).
[48]F. Völklein, H. Reith, and A. Meier, "Measuring methods for the investigation of In-plane and cross-plane thermal conductivity of thin films," Phys. Status Solidi A **210**, 106–118 (2013).
[49]COMSOL Multiphysics, Heat transfer in solids, version 5.2a.
[50]A. C. Ferrari, J. C. Meyer, V. Scardaci, C. Casiraghi, M. Lazzeri, F. Mauri, S. Piscanec, D. Jiang, K. S. Novoselov, S. Roth, and A. K. Geim, "Raman spectrum of graphene and graphene layers," Phys. Rev. Lett. **97**, 187401 (2006).
[51]J. D. Renteria, S. Ramirez, H. Malekpour, B. Alonso, A. Centeno, A. Zurutuza, A. I. Cocemasov, D. L. Nika, and A. A. Balandin, "Strongly anisotropic thermal conductivity of free-standing reduced graphene oxide films annealed at high temperature," Adv. Funct. Mater. **25**, 4664–4672 (2015).